Enhancement of COVID-19 Diagnosis using Machine Learning and Texture Analyses of Lung Imaging

Bhuvan Mittal and JungHwan Oh

Dept. of Comp. Sci. and Eng., University of North Texas, Denton, TX 76203, U.S.A.
Junghwan.Oh@unt.edu

Abstract. Over 186 million cases and 4.0 million deaths from Corona virus were reported worldwide as of July 13, 2021. A multinational consensus from the Fleischner Society reported that Computerized Tomography (CT) can be utilized for the early classification of CT-based Covid-19. However, such diagnosis involves a significant amount of time by radiologists. Automated analysis to classify Covid-19 disease from lung CT will help save radiologists' time and effort. In this paper, we propose 'CoviNet Enhanced', a hybrid approach with a deep three-dimensional convolutional neural network (3D-CNN) and support vector machines (SVMs) to diagnose Covid-19 in CT images, which is an improved version of our previous work 'CoviNet' based on only 3D-CNN. The experimental results show the proposed method is highly effective for Covid-19 detection.

Keywords: Covid-19 detection, Deep learning, Support vector machines, Texture analysis, Lung computerized tomography (CT) scan;

1 Introduction

The Covid-19 is a highly contagious and virulent disease caused by the Severe Acute Respiratory Syndrome - CoronaVirus – 2 (SARS-CoV-2). Over 186 million cases and 4.0 million deaths were reported worldwide as of July 13, 2021 [1]. A multinational consensus from the Fleischner Society reported that Computerized Tomography (CT) can be utilized for the early diagnosis of CT-based Covid-19 [2]. CT also has a high sensitivity in the classification of the Covid-19 disease [3]. However, this binary classification task of identifying Covid-19 positive from negative patients from lung CT involves a significant amount of radiologists' time and effort. Thus, it is crucial to develop an automated analysis of CT images to save radiologists' time in overstretched healthcare environments.

In our previous work [4], we implemented the CoviNet, a 3D CNN-based model for Covid-19 classification of lung CT images. In this paper, we propose an enhancement of this model [4], CoviNet Enhanced using 3D CNN and Leung-Malik (LM) texture features [5] additionally. CoviNet Enhanced has a novel conditional majority voting algorithm with an ensemble of 3D CNN and SVMs, which provides better classification sensitivity and specificity than using the 3D CNN alone [4]. Since the SVM algorithm is complementary, this hybrid approach using SVM models and 3D CNN combined via conditional majority voting shows superior performance.

Contributions of CoviNet Enhanced: To achieve a better classification sensitivity and specificity than those of CoviNet: we add 1) Leung-Malik (LM) texture features [5], 2) an ensemble classifier comprising a 3D CNN and texture features-based SVMs, and 3) conditional majority voting for the final classification.

The remainder of this paper is organized as follows. Related work is presented in Section 2. The proposed method is described in Section 3. In Section 4, we discuss our experimental setup and results. Finally, Section 5 presents some concluding remarks.

2 Related Work

In our previous work [4], we classified the CT images into Covid-19 positive or negative based on the 3D CNN which comprises 3D filters in convolutional layers to train a deep 3D CNN from scratch. This model utilized the 3D CT scan volumes as opposed to individual slice-level CT imaging data to come up with the patient-level diagnosis. It has a network depth of 16 layers comprising four 3D convolutional layers, four 3D max-pooling layers, four 3D batch normalization layers, one global average 3D pooling layer, two fully connected dense layers, one dropout layer, and a final softmax layer. All four convolutional layers have a kernel size of 3×3×3 but use different numbers of kernels at 64, 128, and 256. The RELU activation function is used. The four 3D-max-pooling layers take a 2×2×2 sliding cube which subsamples the image length, width, and depth dimensions and has a stride of 2. To speed up the training of CoviNet, 3D batch normalization layers are included after the 3D pooling layers. Then, 3D global average pooling takes a 4D input of size length × width × depth × channels (= 12×12×2×256) and outputs a one-dimensional output of size 256 channels. Next, the fully connected layer follows with a dimension of 512 followed by a dropout layer with a dropout factor of 0.3 which is introduced to make the model robust to noise. The final softmax layer with sigmoid activation outputs the predicted probability of being Covid-19 positive. Adam optimizer is used with an initial learning rate of 0.001 with an exponential decay rate of 0.96 over 100,000 decay steps.

In Wang et al.'s DeCovNet [6], a single 3D CNN classifier taking only original CTs as input data is implemented for Covid-19 classification into positive and negative classes. In DeCovNet, the 3D convolutional layers are followed by 3D Batch Normalization, Relu activation, and 3D Pooling layers. There are six 3D convolutional layers. Training and testing are done on a proprietary dataset for 100 epochs having an Adam optimizer with a constant learning rate of $1x10^{-5}$.

Imani et al. [7] first used morphological filters to extract the shape and structural features without and with CNN processing. Second, they used Gabor filters to extract textural features without and with the use of a trained CNN for feature extraction. Then they classified the Morphological and Gabor features independently via two separate classifiers: Support Vector Machine and Random Forest. For the Morphological model, the random forest classifier without CNN performed the best, whereas, for the Gabor model, the random forest classifier with trained CNN performed the best.

Goncharov et al. [8] proposed a multitask approach to solving the identification and segmentation tasks together via a 2D U-Net model which outputs a common intermediate feature map that is aggregated into a feature vector via a pyramid pooling layer. The classification layers follow the high-resolution upper part of U-Net and comprise two fully-connected layers followed by a softmax layer which outputs the probability of the input CT volume being Covid-19 positive.

3 Methodology

The proposed approach consists of four components:

(1) 3D CNN:
A 3D CNN having four three-dimensional convolutional kernel layers from our previous work [4] is trained from scratch on the augmented CT data. The augmentation details can be found in our previous work [4], and the 3D CNN architecture was explained in detail in Section 2. It is a deep model with 17 layers comprising four 3D convolutional layers, four 3D max-pooling layers, four 3D batch normalization layers, one global average 3D pooling layer, two fully connected dense layers, one dropout layer, and a final softmax layer. 3D batch normalization layers after the 3D pooling layers help the model learn faster, and the dropout layer contributes to its noise robustness. Early stopping is also invoked if the model loss does not reduce over the last five epochs.

(2) Texture Feature Extraction:
The LM features have textural, shape, and intensity-based features. LM texture features [5] are typically extracted for an image using the 48 LM filters (LM filter bank) which are convolved over the entire input image. The LM filter bank (Figure 1) has a mix of edge, bar, and spot filters at multiple scales and orientations. It has a total of 48 filters - 2 Gaussian derivative filters at 6 orientations and 3 scales, 8 Laplacian of Gaussian filters, and 4 Gaussian filters.

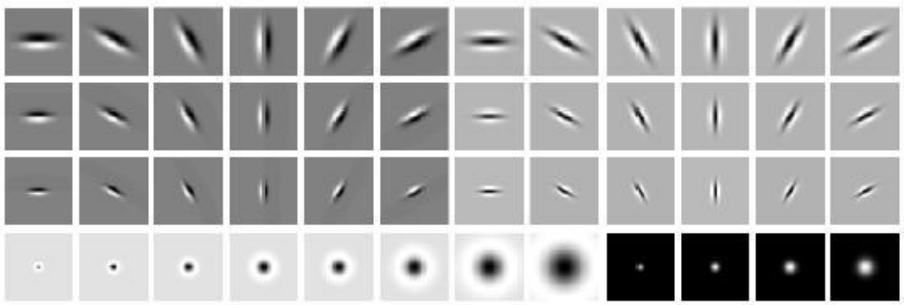

Figure 1. LM filter bank with 48 filters [5].

When we apply the two Gaussian derivative filters at six orientations and three scales shown in the first three rows of Figure 1, we have nearly all-black pixels as a result since lungs do not have elongated objects. The features which can identify

the ground glass opacities and consolidations will be suited for our work. The results of convolving the 12 filters in the bottom row of Figure 1 are shown in Figure 2.

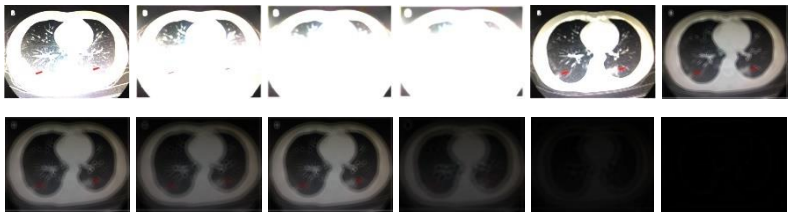

Figure 2. Results of CT image convolving with the 12 filters in the bottom row of Figure 1 (LM37 through LM48)

Intuitively, these are possibly informative features, which can be used for Covid-19 classification. We create 12 separate SVM models taking one feature at a time for all the convolved outputs from the 12 filters. Then, the final feature selection is done by selecting the two top-performing LM filters. The selected top-performing filters are LM37 and LM41 and the results of convolving these filters with the input image are shown in Figure 3.

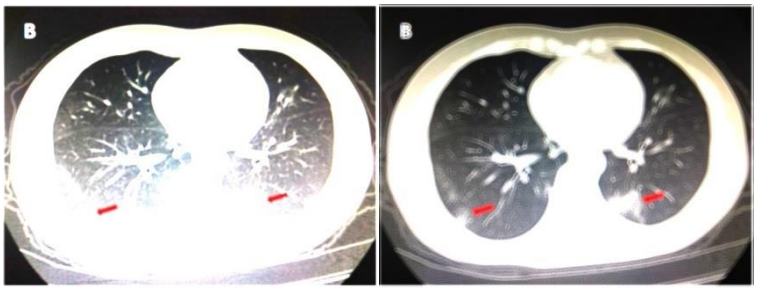

(a) (b)

Figure 3. Results of CT image convolving with the two best-performing LM filters: (a) LM37, and (b) LM41

(3) SVM Models:

The selected LM texture features, namely the LM37 and LM41, along with the original image are classified via three separate SVM classifiers. We use the held-out test dataset approach [9]. 80:20 split is used for training versus testing. First, the original image datasets and the texture feature inputs are resized to 224x224. The Covid-19 CT images with Covid-19 positive or negative physician-provided labels are fed into the first SVM model. The Leung-Malik feature LM41 is used to build the second SVM model. The Leung Malik feature LM37 is used to build the

third SVM model. For the SVM, we perform a grid search for the parameter values of 'C' of 1, 10, 100, 1000, with a linear kernel for efficiency, and with gamma values of 0.001 and 0.0001 with the Radial Basis Function kernel. We then get the predicted class for each image in the test dataset. This is repeated over the five folds.

(4) Ensemble of 3D CNNs and SVMs

We found that the 3D CNN predictions have a positive class probability that varies for each input ranging from 0.1% to 99.9%. For some inputs, our 3D CNN does have an uncertain prediction with Covid-19 positive class probability values (between 46% and 54%). In such cases, our 3D CNN is not very confident about the prediction. To improve the predictions for this range, we use conditional majority voting to combine the predicted outputs of the 3D CNN with the three SVMs.

When the original 3D CNN's prediction has a probability in a certain range i.e., between the low threshold (Th_{Low}: 46% in our case) and the high threshold (Th_{High}: 54% in our case), then the model uses the LM Texture-features' SVM model predictions along with 3D CNN via majority voting to make the final classification. When the original 3D CNN's prediction has a probability smaller than the low threshold (Th_{Low}: 46% in our case) or larger than the high threshold (Th_{High}: 54% in our case), only the 3D CNN's output makes the final classification. These probability threshold values were determined by experiments and fine-tuned on the validation dataset. This gives the final predicted classification of Covid-19 positive or Covid-19 negative. The model performance is evaluated based on comparing this final prediction on held-out test data with the ground truth labels. The detailed architecture of CoviNet Enhanced is shown in Figure 4. The conditional majority voting algorithm is showcased in Figure 5.

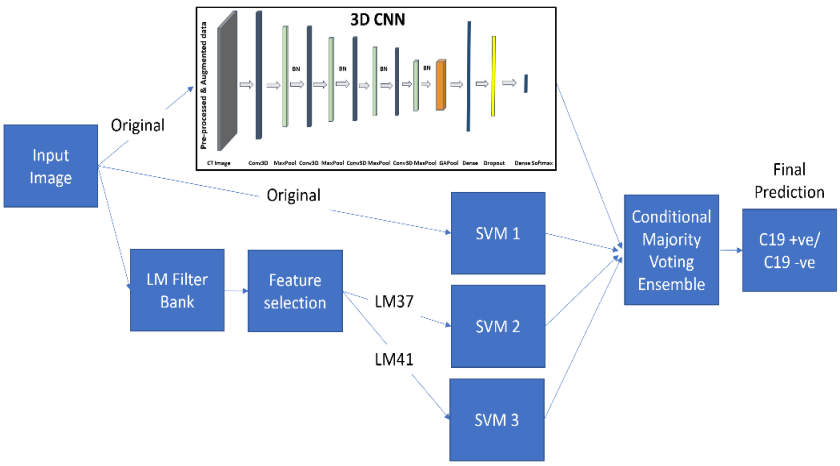

Figure 4. Ensemble classifier of 3D CNNs and Support Vector Machines based on texture features.

Algorithm 1 Conditional Majority Voting Rule for Classification

Inputs: 3D CNN's positive class probability (C), first SVM's positive class probability (S1), second SVM's positive class probability (S2), third SVM's positive class probability (S3)

if 0.46 < C < 0.54 then

'final predicted positive class probability' ← (C+S1+S2+S3)/4

else

'final predicted positive class probability' ← C

end if

Figure 5. Algorithm for conditional majority voting rule for classification.

4 Experiments and Results

CoviNet Enhanced was implemented in 'jupyter-notebook' using python's 'tensorflow', 'keras', and other libraries [9, 10, 11, 12, 13]. The pre-processing of the data was done using the 'nibabel' library for medical image processing which can read the CT volume data provided in .nii format [14]. Data augmentation was performed on the entire dataset using the 'scipy' and 'ndimage' libraries. The augmentation details can be found in our previous work [4].

The dataset was split 80:20 for training and validation, and each patient's images are either entirely in the training dataset or entirely in the validation dataset. Five-folds are used for cross-validation as discussed earlier. Adam optimizer with an exponentially decaying learning rate and an initial learning rate of 0.0001 with a decay rate of 0.96, and with 100,000 decay steps was used. The training was done with an upper limit of 100 epochs with an early stopping criterion based on validation accuracy not improving over the next five epochs.

We trained and evaluated our CoviNet Enhanced model's performance on UCSD-AI4H [15], MosMed [16], and MosMed_selected on lung CT datasets described in Tables 1, 2, and 3 respectively. Since the MosMed dataset in Table 2 is very large, we selected some of them for faster evaluations, which is shown in Table 3.

Table 1. UCSD-AI4H dataset [15]

Class	Training	Validation
Covid-19 Positive	172 patients 279 images	41 patients 70 images
Covid-19 Negative	140 patients 317 images	31 patients 80 images

Table 2. MosMed dataset.

Class	Train	Validation	Test	Totals
Covid-19 Positive	582 patients 14,681 images	102 patients 2,573 images	172 patients 4,339 images	856 patients 21,593 images
Covid-19 Negative	173 patients 4,321 images	30 patients 749 images	51 patients 1,337 images	254 patients 6,407 images
Overall	**755 patients** **19,002 images**	**132 patients** **3,322 images**	**223 patients** **5,676 images**	**1,110 patients** **28,000 images**

Table 3. MosMed_selected dataset

Class	Train	Validation
Covid-19 Positive	138 patients 3,385 images	34 patients 860 images
Covid-19 Negative	203 patients 5,305 images	51 patients 1,337 images

The various performance metrics to evaluate our model's performance are accuracy, sensitivity (recall), specificity, precision, F-score, and Matthew's correlation coefficient (MCC) [17]. These metrics are defined as follows in equations (1), (2), (3), (4), (5) and (6):

$$\text{Accuracy} = \frac{(TP + TN)}{(TP + TN + FP + FN)} \tag{1}$$

$$\text{Sensitivity (Recall)} = \frac{(TP)}{(TP + FN)} \tag{2}$$

$$\text{Specificity} = \frac{(TN)}{(TN + FP)} \tag{3}$$

$$\text{Precision} = \frac{(TP)}{(TP + FP)} \tag{4}$$

$$\text{F1} = \frac{(2 \times Precision \times Recall)}{(Precision + Recall)} = \frac{(2 \times TP)}{(2 \times TP + FP + FN)} \tag{5}$$

$$\text{MCC} = \frac{(\text{TP} \times \text{TN} - \text{FP} \times \text{FN})}{\sqrt{((\text{TP} + \text{FP})(\text{TP} + \text{FN})(\text{TN} + \text{FP})(\text{TN} + \text{FN}))}} \tag{6}$$

where TP, TN, FP, and FN stand for Covid-19 positive patients predicted as Covid-19 positive, Covid-19 negative patients predicted as Covid-19 negative, Covid-19 negative patients predicted as Covid-19 positive, and Covid-19 positive patients predicted as Covid-19 negative, respectively.

To perform a fair comparison against previously published work, we also re-implemented Wang et al.'s DeCovNet [6] on the three datasets in this paper. We trained and evaluated Wang et al.'s DeCovNet [6] model's performance on UCSD-AI4H [15],

MosMed [16], and MosMed_selected on lung CT datasets described in Tables 1, 2, and 3 respectively.

On the UCSD-AI4H dataset, the performance comparison of CoviNet Enhanced with previously published works, namely, Wang et al.'s DeCovNet [6], Imani et al.'s Gabor, and Morphological models [7] is shown in Table 4. For Imani's Gabor model, the random forest classifier with CNN feature extraction was used, and for Imani's Morphological model, the random forest classifier alone was used. Imani et al.'s [7] also used the UCSD-AI4H dataset for their Covid-19 classification from CT, so we report their best-performing results (for Gabor and Morphological models) directly from their paper.

Among all the four models shown in Table 4, CoviNet Enhanced exhibited the highest F1-score of 0.930 and the MCC of 0.842 on the UCSD-AI4H dataset. Further, CoviNet Enhanced showed significantly superior performance than the next best-performing model, Wang et al.'s DeCovNet [6], which had an F1-score of 0.861, and an MCC of 0.717.

Table 4. Performance Comparison between CoviNet Enhanced and other published works on the UCSD-AI4H dataset (Table 1).

Model	Accuracy	Precision	Sensitivity	Specificity	F1-score	MCC
Wang et al.'s DeCovNet [6]	85.5%	91.9%	80.9%	91.2%	0.861	0.717
Imani's Gabor [7]	76.7%	-	-	-	0.743	-
Imani's Morphological [7]	75.3%	-	-	-	0.753	-
CoviNet Enhanced	**92.2%**	**93.0%**	**93.0%**	**91.2%**	**0.930**	**0.842**

On the MosMed dataset, the performance comparison of CoviNet Enhanced with Wang et al.'s DeCovNet [6] is shown in Table 5. Among the two models shown in Table 5, CoviNet Enhanced exhibited the highest F1-score of 0.774 and the MCC of 0.608 on the MosMed_selected dataset. Further, CoviNet Enhanced showed significantly superior performance than the next best-performing model, Wang et al.'s DeCovNet [6], which had an F1-score of 0.652, and MCC of 0.353.

The reason for CoviNet Enhanced's superior performance over DeCovNet is the ensemble approach which leverages the complementary texture features based SVM models when 3D CNN is less confident in its prediction.

On the MosMed_selected dataset, the performance comparison of CoviNet Enhanced with Goncharov et al.'s [8] model is shown in Table 6. Goncharov et al.'s [8] also used this same dataset, so the results are reported directly from their paper. CoviNet Enhanced exhibited the highest F1-score of 0.957 and the MCC of 0.926.

Table 5. Performance Comparison between CoviNet Enhanced and the other published work on MosMed dataset (Table 2).

Model	Accuracy	Precision	Sensitivity	Specificity	F1-score	MCC
Wang et al.'s DeCovNet [6]	66.8%	74.1%	58.3%	76.7%	0.652	0.353
CoviNet Enhanced	**80.8%**	**75.7%**	**79.1%**	**82.0%**	**0.774**	**0.608**

Further, CoviNet Enhanced showed significantly superior performance than the next best model, Goncharov et al.'s multitasksp1 U-Net [8], which had an F1-score of 0.827, and MCC of 0.770. Goncharov et al's method involved multitask learning by jointly learning to classify and segment, and it was very slow to train versus our relatively more efficient CoviNet Enhanced 3D CNN classification.

Table 6. Performance Comparison between CoviNet Enhanced and Goncharov et al. [8] on MosMed_selected dataset (Table 3).

Model	Accuracy	Precision	Sensitivity	Specificity	F1-score	MCC
Goncharov et al. multitask-sp1 U-Net [8]	89.4%	72.1%	96.9%	86.8%	0.827	0.770
CoviNet Enhanced	**96.4%**	**94.3%**	**97.1%**	**95.9%**	**0.957**	**0.926**

The performance comparison of CoviNet [4] (our previous work) and CoviNet Enhanced is shown in Table 7. On the UCSD-AI4H dataset, CoviNet Enhanced outperforms the CoviNet by 1.3% on Sensitivity, 32.9% on Specificity, 0.144 on F1-score, and 0.312 on MCC. Notably, CoviNet Enhanced has the highest F1-score and MCC score at 0.930 and 0.842 respectively versus CoviNet's F1-score and MCC of 0.786 and 0.530. On the MosMed_selected dataset, CoviNet Enhanced outperforms the CoviNet by 3.7% on Specificity, 0.027 on F1-score, and 0.044 on MCC as shown in Table 7. Notably, CoviNet Enhanced has a higher F1-score and MCC score at 0.957 and 0.926 respectively versus CoviNet's F1-score and MCC of 0.930 and 0.882.

We now show the result of feeding the entire 3D volume of a patient's CT compares with utilizing each image in isolation using the same 3D CNN CoviNet Enhanced approach. The proposed CoviNet Enhanced model's 3D CNN component takes only 3D CT volumes since the 3D CNN processes the entire 3D volume together and makes predictions at volume level only. Note that the SVMs take image-level data and the SVM predictions are averaged for the images constituting a volume to get the final volume level predictions. To get image-level results from 3D CNN, we provided input as a single CT slice duplicated five times to make volume data for feeding to the 3D CNN. Table 8 shows the image-level and patient-level metrics of the CoviNet Enhanced model on the UCSD-AI4H dataset.

Table 7. Performance Comparison between CoviNet and CoviNet Enhanced on UCSD-AI4H (Table 1) and MosMed_selected (Table 3).

Model/Data	Accuracy	Precision	Sensitivity	Specificity	F1-score	MCC
CoviNet /UCSDAI4H	75.0%	68.7%	91.7%	58.3%	0.786	0.530
CoviNet Enhanced/ UCSD-AI4H	**92.2%**	**93.0%**	**93.0%**	**91.2%**	**0.930**	**0.842**
CoviNet /MosMed_selected	94.1%	89.2%	97.1%	92.2%	0.930	0.882
CoviNet Enhanced/ MosMed_selected	**96.4%**	**94.3%**	**97.1%**	**95.9%**	**0.957**	**0.926**

Table 8. Image-level and patient-level metrics of CoviNet Enhanced.

CoviNet Enhanced	Accuracy	Precision	Sensitivity	Specificity	F1-score	MCC
Patient-Level (3D volume-level)	92.2%	93.0%	93.0%	91.2%	0.930	0.842
Image-Level	72.1%	100.0%	60.0%	100.0%	0.750	0.559

As shown in Table 8, CoviNet Enhanced patient-level outperforms the CoviNet Enhanced Image-Level by 33.0% on Sensitivity, 0.180 on F1-score, and 0.283 on MCC although it does have an 8.8% lower Specificity. The increased sensitivity of the CoviNet Enhanced patient-level model versus the image-level model is much higher than the lowered specificity. CoviNet Enhanced patient-level has a higher F1-score and MCC score at 0.930 and 0.842 versus the CoviNet Enhanced image-level model with an F1-score and MCC of 0.750 and 0.559, respectively.

The results show the power of learning from the sequential nature of the consecutive slices in a CT volume. If the disease prediction is uncertain in one slice, the corresponding slices in the vicinity will help provide greater context and help improve the performance. Even noisy pixels occurring due to random noise will not occur in the same place in consecutive slices, so the model will become more robust to noise and be able to learn better. Therefore, learning from 3D volumes is better, in that the model learns from not only the spatial dimension but also the depth dimension.

We now compare the 3D CoviNet Enhanced model with a comparable 2D model. For the CNN part of the CoviNet Enhanced model, the 3D input CT volumes, 3D convolutional, and 3D pooling layers are replaced by 2D CT input images, 2D convolutional, and 2D pooling layers, respectively. The 3D layers of the 3D CNN have 4 dimensions of length×width×depth×channels, but the corresponding 2D layers of the 2D CNN have

3 dimensions of length×width×channels only. The SVM portion of the CoviNet Enhanced model remains unchanged. Table 9 shows the CoviNet Enhanced's performance on UCSD-AI4H with 3D CNN versus 2D CNN in which 3D CNN is around 10 to 20% better on the various performance measures than 2D CNN.

Table 9. Performance of CoviNet Enhanced on UCSD-AI4H with 3D versus 2D CNN

Model	Accuracy	Precision	Sensitivity	Specificity	F1-score	MCC
2D CNN	77.10%	76.67%	73.64%	80.13%	0.750	0.541
3D CNN	92.2%	93.0%	93.0%	91.2%	0.930	0.842

5 Concluding Remarks

Automated Covid-19 diagnosis via deep learning on lung CT is highly sensitive in detecting Covid-19 disease-induced pneumonic changes [18]. The proposed CoviNet Enhanced model with a hybrid approach is an excellent diagnostic model for Covid-19 diagnosis for lung CT as it exhibits not only high sensitivity but also high specificity. It achieved the higher performance because it utilizes both a deep 3D convolutional neural network and Leung-Malik texture features-based SVMs. It outperforms the CoviNet, our previous work [4] because of the hybrid approach and our novel conditional majority voting ensemble approach. In the instances where the 3D CNN is uncertain about its Covid-19 prediction, the texture features-based SVMs help to complement the 3D CNN. The SVM is a non-neural network method and hence it serves as a complementary technique to the 3D CNN. This hybrid approach of deep learning with textural features and conditional majority voting helps to overcome the weakness of the 3D CNN alone. The experimental results show the proposed method is highly effective for Covid-19 detection.

Our approach will not only save the radiologist's time but also improve the diagnostic performance in terms of much higher sensitivity and similar specificity. Our model achieved its best sensitivity of 97.1% and a specificity of 95.9%. In comparison, a radiologists' performance study in differentiating Covid-19 from other viral pneumonia reported that the median values of sensitivity and specificity were 83% (ranging 67%-97%) and 96.5% (ranging 7%-100%), respectively [19].

For future work, to further improve the model performance, a larger and higher resolution dataset should be leveraged which will allow for reliable training of a deeper and more complex model. A temporal study of how the Covid-19 disease manifestation changes would also be helpful. The three-way classification to distinguish non-viral or bacterial pneumonia from Covid-19 also merits further research.

References

1. Weekly epidemiological update on COVID-19—13 July 2021. (n.d.). Retrieved July 22, 2021, from https://www.who.int/publications/m/item/weekly-epidemiological-update-on-covid-19---13-july-2021
2. Rubin GD, Ryerson CJ, Haramati LB, Sverzellati N, Kanne JP, Raoof S, et al. The Role of Chest Imaging in Patient Management during the COVID-19 Pandemic: A Multinational Consensus Statement from the Fleischner Society. Radiology 2020 Jul;296 (1):172-180
3. https://radiologyassistant.nl/chest/covid-19/covid19-imaging-findings
4. Mittal B., Oh J. CoviNet: Covid-19 Diagnosis using Machine Learning Analyses for Computerized Tomography Images. The 13th International Conference on Digital Image Processing (ICDIP 2021), Singapore, May 20-23, 2021.
5. Varnousfaderani, E. S., Yousefi, S., Bowd, C., Belghith, A., & Goldbaum, M. H. (2015). Vessel Delineation in Retinal Images using Leung-Malik filters and Two Levels Hierarchical Learning. AMIA Annual Symposium proceedings. AMIA Symposium, 015, 1140–1147.
6. Wang, X., Deng, X., Fu, Q., Zhou, Q., Feng, J., Ma, H., Liu, W., & Zheng, C. (2020). A Weakly-Supervised Framework for COVID-19 Classification and Lesion Localization From Chest CT. IEEE Transactions on Medical Imaging, 39(8), 2615–2625. https://doi.org/10.1109/TMI.2020.2995965
7. Imani, M. (2021). Automatic diagnosis of coronavirus (COVID-19) using shape and texture characteristics extracted from X-Ray and CT-Scan images. Biomedical Signal Processing and Control, 68, 102602.
8. Goncharov, M., Pisov, M., Shevtsov, A., Shirokikh, B., Kurmukov, A., Blokhin, I., Chernina, V., Solovev, A., Gombolevskiy, V., Morozov, S., & Belyaev, M. (2021). CT-based Covid-19 Triage: Deep Multitask Learning Improves Joint Identification and Severity Quantification. Medical Image Analysis, 102054.
9. Bernico, M. (2018). Deep learning quick reference: Useful hacks for training and optimizing deep neural networks with tensorflow and keras. Chapter 1, pp. 23.
10. Harris, C. R., Millman, K. J., van der Walt, Stéfan J, Gommers, R., Virtanen, P., Cournapeau, D., Wieser, E., Taylor, J., Berg, S., Smith, N. J., Kern, R., Picus, M., Hoyer, S., van Kerkwijk, M. H., Brett, M., Haldane, A., Del Río, J. F., Wiebe, M., Peterson, P., . . . Oliphant, T. E. (2020). Array programming with NumPy. Nature (London), 585(7825), 357-362.
11. Hunter, J. D. (2007). Matplotlib: A 2D graphics environment. Computing in Science & Engineering, 9(3), 90-95.
12. https://scikit-learn.org/stable/index.html
13. https://jupyter.org
14. https://libraries.io/pypi/nibabel
15. Yang, X., He, X., Zhao, J., Zhang, Y., Zhang, S., & Xie, P. (2020). Covid-CT-Dataset: A CT Scan Dataset about Covid-19. ArXiv:2003.13865 [Cs, Eess, Stat].
16. Morozov S.P., Andreychenko A.E., Blokhin I.A., Gelezhe P.B., Gonchar A.P., Nikolaev A.E., Pavlov N.A., Chernina V.Y., Gombolevskiy V.A., (2020). MosMedData: Data set of 1110 chest CT scans performed during the Covid-19 epidemic. Digital Diagnostics, 1(1), 49–59.
17. D. Chicco and G. Jurman, “The advantages of the Matthews correlation coefficient (MCC) over F1 score and accuracy in binary classification evaluation,” BMC Genomics, vol. 21, no. 1, p. 6, Dec. 2020.

18. Rubin GD, Ryerson CJ, Haramati LB, Sverzellati N, Kanne JP, Raoof S, et al. The Role of Chest Imaging in Patient Management during the Covid-19 Pandemic: A Multinational Consensus Statement from the Fleischner Society. Radiology 2020 Jul;296 (1):172-180
19. Bai, H. X., Hsieh, B., Xiong, Z., Halsey, K., Choi, J. W., Tran, T. M. L., Pan, I., Shi, L.-B., Wang, D.-C., Mei, J., Jiang, X.-L., Zeng, Q.-H., Egglin, T. K., Hu, P.-F., Agarwal, S., Xie, F.-F., Li, S., Healey, T., Atalay, M. K., & Liao, W.-H. (2020). Performance of Radiologists in Differentiating COVID-19 from non-COVID-19 Viral Pneumonia at Chest CT. Radiology, 296(2), E46–E54. https://doi.org/10.1148/radiol.2020200823